The lubrication mechanisms of textured surfaces

Tribology Today, Istanbul

Noël Brunetière

April 18, 2026

Institut Pprime, Poitiers, France

Fluid flow in a lubricated contact and load carrying capacity

Pressure flow (Hydrostatic effect)

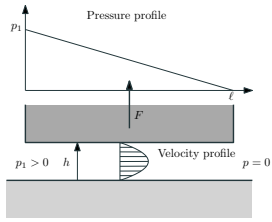

- The mass flow rate per unit length is $\dot{m} = \frac{\rho}{12\mu}\frac{p_1}{\ell}h^3$.
- Very strong impact of h on the flow.
- Constant force per unit length is $F = \frac{p_1}{2}\ell$.

Shear flow (Hydrodynamic effect)

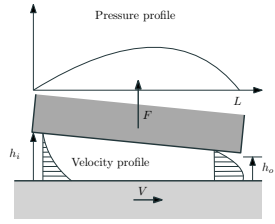

- Force per unit length is $F = \frac{6\mu V L^2}{h_o^2}\left[\frac{\ln K}{(K-1)^2} - \frac{2}{K^2-1}\right]$ with $K = \frac{h_i}{h_o}$
- Positive force can be generated depending on the slope. Zero force with $K = 1$ (flat on flat)

Lubrication regimes

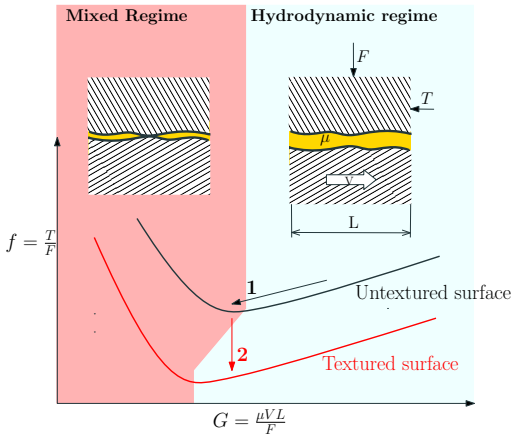

Friction reduction

- Reduce G:
- Reduce size L or viscosity μ
- Risk of mixed lubrication and contact
- More particularly for flat on flat surfaces
- Surface texturing

Surface texturing[1],[2]

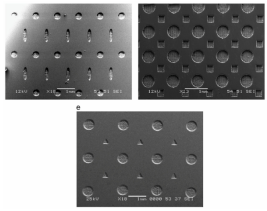

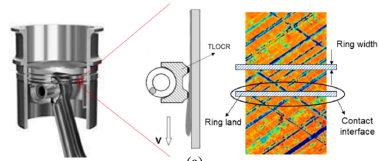

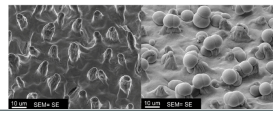

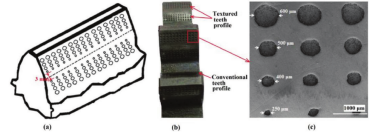

[1]Philipp G. Grützmacher, Francisco J. Profito, and Andreas Rosenkranz. **"Multi-Scale Surface Texturing in Tribology-Current Knowledge and Future Perspectives".** In: *Lubricants* 7.11 (2019). DOI: 10.3390/lubricants7110095.

[2]Andreas Rosenkranz et al. **"Surface Texturing in Machine Elements - A Critical Discussion for Rolling and Sliding Contacts".** In: *Advanced Engineering Materials* 21.8 (2019), p. 1900194. DOI: 10.1002/adem.201900194.

Pioneering work[3]

- Origin of the load support in flat on flat lubrication
- Role of micro-irregularities (asperities)
- Experimental analysis of artificial rough surface
- Network of bumps by photo-etching
- Fluid film formation and load support due to surface texture

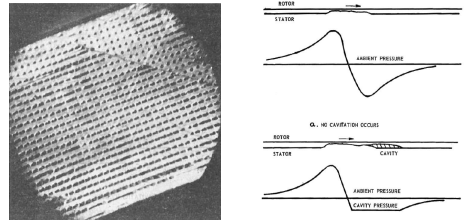

a) b)

Figure 1: a) Surface texture used by Hamilton et al. and b) proposed load support mechanism

[3]D.B. Hamilton, J.A. Walowit, and C.M. Allen. **"A Theory of Lubrication by Micro-irregularities".** In: *Journal of Basic Engineering* 88 (1966), pp. 177–185.

Literature

- No publication during about 30 years
- Development of surface texturing by laser and other technics in the 90'
- Increasing interest

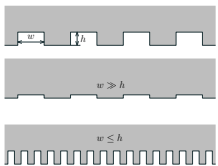

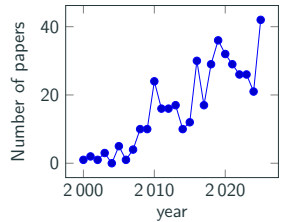

Figure 2: Number of papers: Google Scholar "allintitle: surface (texturing OR texture OR textured) (lubrication OR lubricated OR hydrodynamic)"

Example 1: shallow grooves[4]

- Friction of mechanical seals (flat on flat annular lubricated contact)
- texturing by ion-etching through a mask
- More than 50 % of friction reduction and no wear

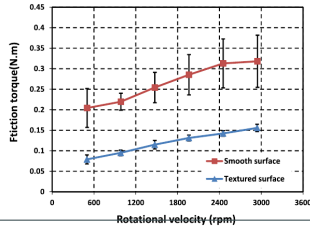

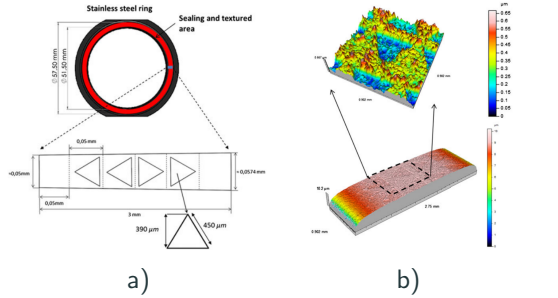

Figure 3: a) Configuration of the contact and surface texture and b) Topography of the surface

[4] M. Adjemout, N. Brunetière, and J. Bouyer. **"Friction and temperature reduction in a mechanical face seal by a surface texturing: comparison between TEHD simulations and experiments".** In: *Tribology Transactions* 61.6 (2018), pp. 1084–1093. DOI: 10.1080/10402004.2018.1478053. URL: https://doi.org/10.1080/10402004.2018.1478053.

Example 2: deep grooves[5]

- Deep and narrow cavities / pillars
- Super-hydrophobic surface, poor wetting
- Allow apparent slip of the liquid, reduce friction

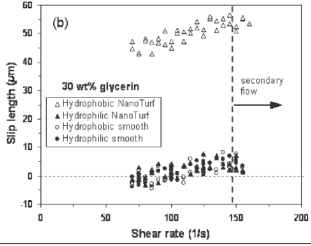

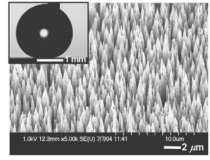

a)

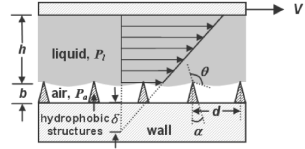

b)

Figure 4: a) Surface texture and wetting b) Slip of the fluid

[5]Chang-Hwan Choi and Chang-Jin Kim. **"Large Slip of Aqueous Liquid Flow over a Nanoengineered Superhydrophobic Surface".** In: *Phys. Rev. Lett.* 96 (6 2006), p. 066001. DOI: 10.1103/PhysRevLett.96.066001.

Outline of the course

1. Shallow grooves
   - Lubrication of one cavity
   - Multiple cavities in bearings
   - Multiple cavities in seals
   - Conclusions
2. Deep grooves
   - Wetting of surfaces
   - Effect of surface topography
   - Flow over one cavity
   - Multiple cavities
   - Multiple cavities
   - Conclusions
3. Conclusions

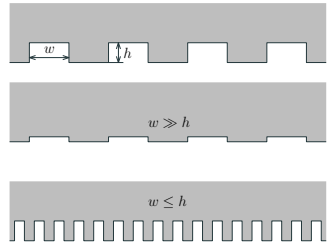

Shallow grooves

Step bearing

- Lubrication assumptions ($h \ll L$)
- Reynolds equation:
- $\frac{\partial}{\partial x}\left(\frac{\rho h^3}{12\mu}\frac{\partial p}{\partial x}\right) = \frac{U}{2}\frac{\partial \rho h}{\partial x}$
- $\bar{h} = \frac{h_t}{h_f}$
- Solution: $p_m = \frac{3\mu UL}{h^2} \times \frac{\bar{h}-1}{\bar{h}^3+1}$

- Pressure $\propto L$
- h_t must be close to $2 \times h_f$
- No effect for deep grooves

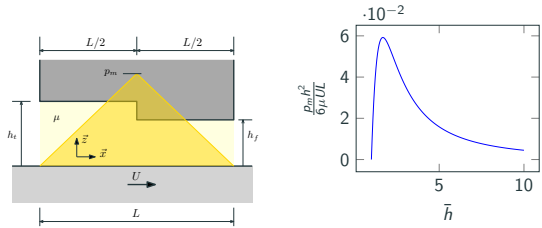

a) b)

Figure 5: a) Configuration of a step bearing b) Max pressure

One centered cavity

- Lubrication assumptions ($h \ll L$)
- Reynolds equation:
- $\frac{\partial}{\partial x}\left(\frac{\rho h^3}{12\mu}\frac{\partial p}{\partial x}\right) = \frac{U}{2}\frac{\partial \rho h}{\partial x}$

- Anti-symmetrical pressure distribution
- No load generation

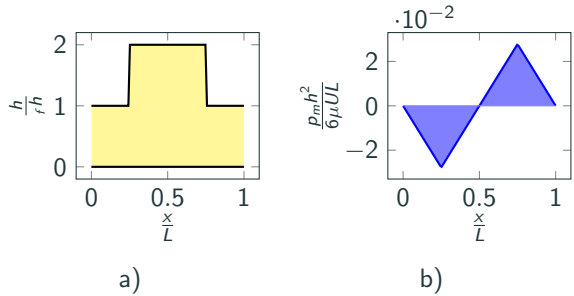

Figure 6: a) Film thickness distribution b) Pressure distribution

One centered cavity with cavitation

- Occurrence of cavitation:
- In cavitation zone: $p = p_c$
- In cavitation zone: $\rho \leq \rho_\ell$ where ρ_ℓ is the lubricant density

- No symmetry in the pressure distribution
- $p_c = -0.01 \frac{6\mu UL}{h^2}$
- Negative load
- $p_{av} = \frac{1}{L}\int_0^L p dx = -0.0033 \times \frac{6\mu UL}{h^2}$

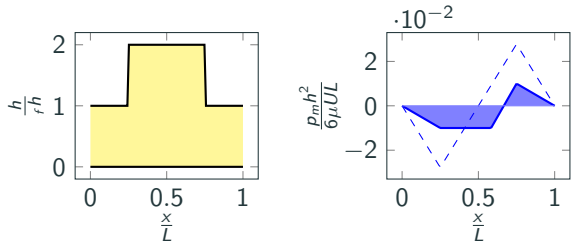

Figure 7: a) Film thickness distribution b) Pressure distribution

One cavity not centered

- The cavity is not in the center of the contact
- Cavitation pressure $p_c = -0.01\frac{6\mu UL}{h^2}$

- No symmetry in the pressure distribution
- **Positive load**
- $p_{av} = -0.0136 \times \frac{6\mu UL}{h^2}$

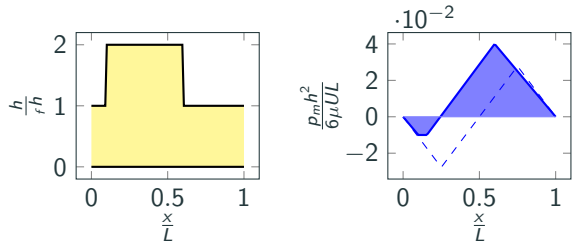

Figure 8: a) Film thickness distribution b) Pressure distribution

Slider bearing[6]

- Slider bearing partially textured at the inlet
- Full texturing = one cavity, no load

- Pressure generation
- Less efficient than an equivalent step bearing
- Limited interest

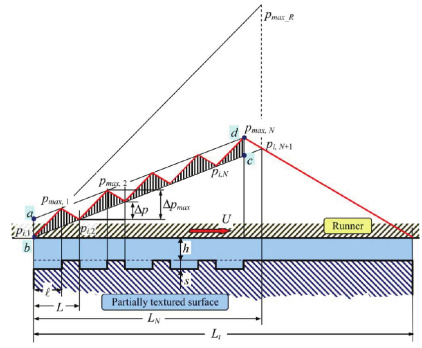

Figure 9: Configuration of the problem and pressure distribution

[6] M D Pascovici et al. **"Analytical investigation of a partially textured parallel slider".** In: *Proceedings of the Institution of Mechanical Engineers, Part J: Journal of Engineering Tribology* 223.2 (2009), pp. 151–158. DOI: 10.1243/13506501JET470. URL: https://doi.org/10.1243/13506501JET470.

Thrust bearing[7]

- Thrust bearings with partial texturing and pocket

- Better efficiency of the pockected bearing

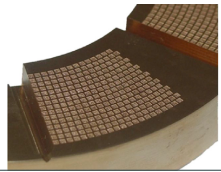

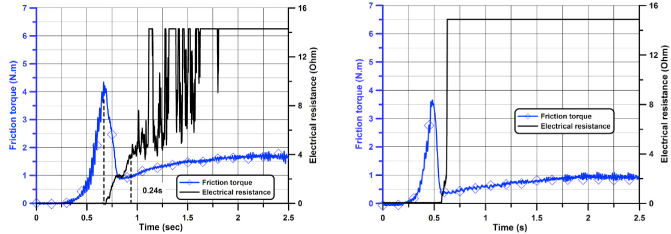

Figure 10: Friction torque and contact resistance for a) textured bearing b) pocketed bearing

[7] Y. Henry, J. Bouyer, and M. Fillon. **"Experimental analysis of the hydrodynamic effect during start-up of fixed geometry thrust bearings".** In: *Tribology International* 120 (2018), pp. 299–308. ISSN: 0301-679X. DOI: https://doi.org/10.1016/j.triboint.2017.12.021. URL: https://www.sciencedirect.com/science/article/pii/S0301679X17305790.

Principle of a mechanical seal

2 flat and smooth surfaces to close the gap

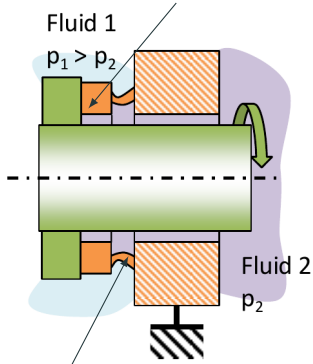

A flexible link to align the surfaces

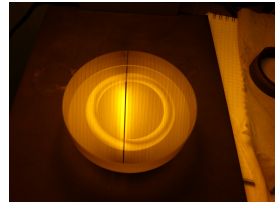

Figure 11: Surface flatness $\approx 0.3\ \mu$m

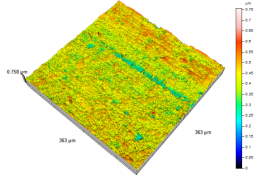

Figure 12: Surface roughness, Sq $= 0.05\ \mu$m

Mechanical seal[8]

- Mechanical seal with one row of cavities
- Periodical boundary conditions

- Limited load generation
- Triangle provides negative load and significant radial flow

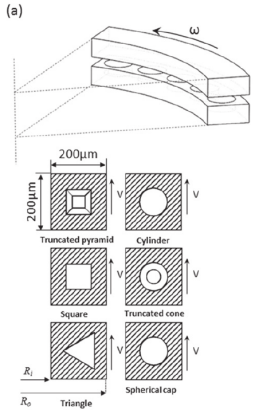

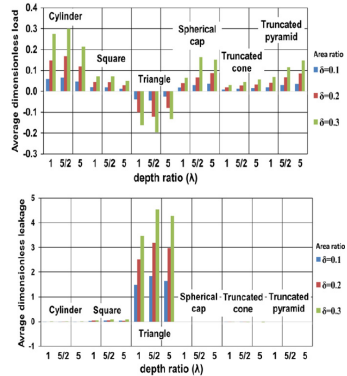

Figure 13: Load and leakage with the different configurations

[8] M Adjemout, N Brunetiere, and J Bouyer. **"Numerical analysis of the texture effect on the hydrodynamic performance of a mechanical seal".** In: *Surface Topography: Metrology and Properties* 4.1 (2016), p. 014002. DOI: 10.1088/2051-672X/4/1/014002.

Mechanical seal[9]

- Mechanical seal with two rows of cavities
- Periodical boundary conditions

- Triangles very efficient compared to other types
- Collective effect thanks to opposite radial flows

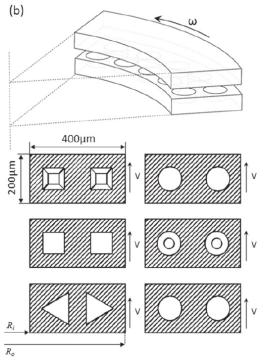

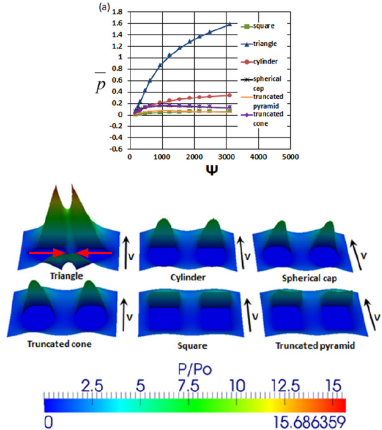

Figure 14: Load and pressure with the different configurations

[9] Adjemout, Brunetiere, and Bouyer, "Numerical analysis of the texture effect on the hydrodynamic

Example 1: shallow grooves[10]

- Friction of mechanical seals (flat on flat annular lubricated contact)
- texturing by ion-etching through a mask
- More than 50 % of friction reduction and no wear

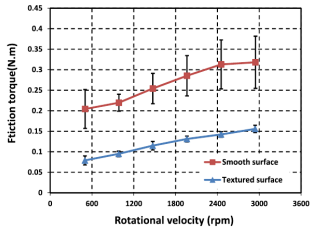

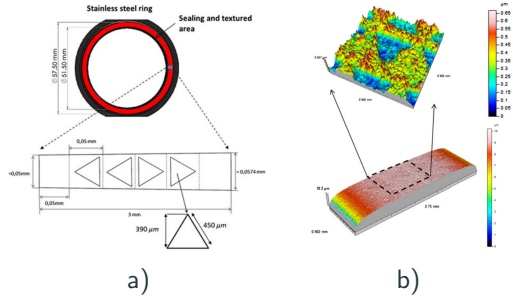

Figure 15: a) Configuration of the contact and surface texture and b) Topography of the surface

[10] Adjemout, Brunetière, and Bouyer, "Friction and temperature reduction in a mechanical face seal by a surface texturing: comparison between TEHD simulations and experiments".

Comparison to other texture types[11]

- The other symmetrical texture should be bad !!
- Let's try !

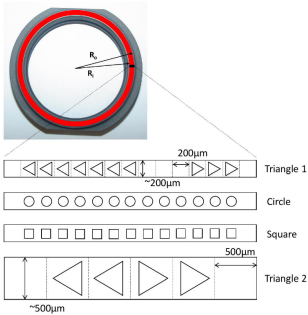

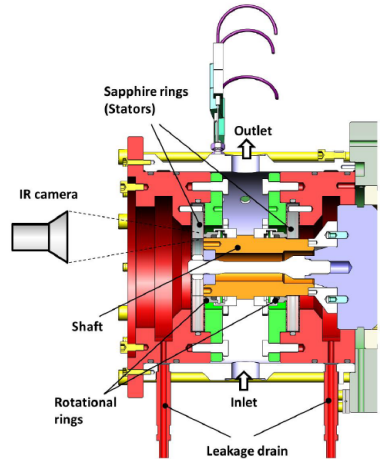

Figure 16: Test cell and temperature measurement

[11] Kacou Dingui et al. **"Surface Texturing to Reduce Temperature in Mechanical Seals".** In: *Tribology Online* 15.4 (2020), pp. 222–229. DOI: 10.2474/trol.15.222.

Comparison to other texture types[12]

centering

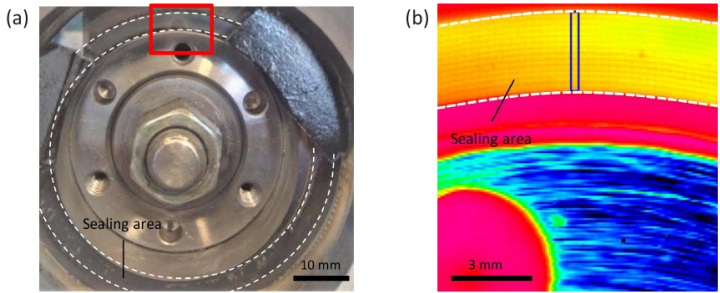

Fig. 5 a) View of the front of the test cell -b) Infrared view within the red square. The blue rectangle corresponds to the area analyzed to calculate the temperature.

[12]Dingui et al., "Surface Texturing to Reduce Temperature in Mechanical Seals".

Comparison to other texture types[13]

- Good results with other textures (symmetrical ones)
- Temperature controlled by texture area not the shape !!
- Why ??

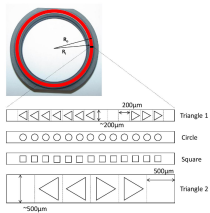

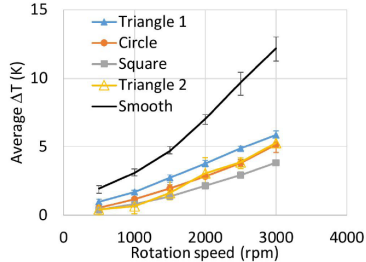

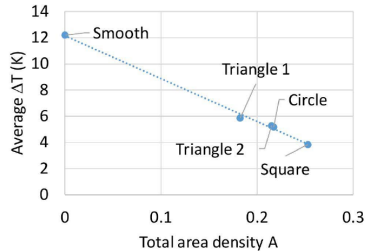

Figure 17: Main results

Why symmetrical texture works in seals?[14]

- Mechanical seal with 19 rows of spherical cap cavities
- Mixed lubrication model

- Rough surfaces can reach hydrodynamic regime
- Texturing improve this capability

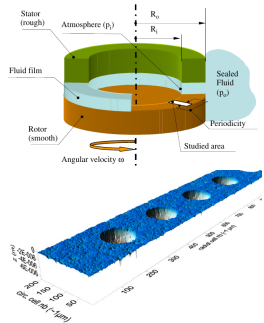

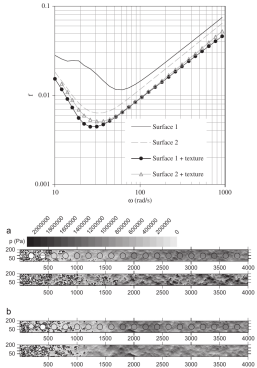

Figure 18: Stribeck curves and pressure distribution for rough and rough textured surfaces

[14] N. Brunetière and B. Tournerie. **"Numerical Analysis of a Surface-Textured Mechanical Seal Operating in Mixed Lubrication Regime".** In: *Tribology International* 49 (2012), pp. 80–89. URL: https://doi.org/10.1016/j.triboint.2012.01.003.

Conclusion on shallow grooves

- Can surface texturing with shallow grooves help in flat on flat lubrication ?
- **Yes** by enhancing hydrodynamic pressure generation **but with conditions**
- Bearing like configurations:
  - Partial texturing located at the inlet only
  - However less efficient than a pocket (step bearing)
- Seal like configurations (flat ring on flat ring):
  - Triangular cavities placed base to base can provide a collective effect and load generation
  - No collective effect with symmetrical cavities
  - Symmetrical cavities can improve the natural pressure generation due to surface roughness
- Cavitation is not the mechanism that make surface texture working

Deep grooves

Contact angle: Energetic approach

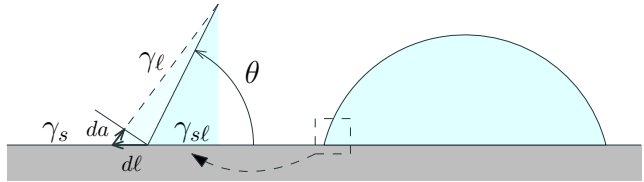

Figure 19: Energy balance at equilibrium

- Liquid surface energy variation $da\gamma_\ell$
- Solid surface energy variation $-d\ell\gamma_s$
- Solid liquid interfacial energy variation $d\ell\gamma_{s\ell}$
- At equilibrium the energy is minimzed, small variation must vanish
- $da\gamma_\ell + d\ell\gamma_{s\ell} - d\ell\gamma_s = 0$
- Geometric relation: $da = \cos\theta d\ell$
- Young's equation: $\gamma_\ell \cos\theta = \gamma_s - \gamma_{s\ell}$

Different surface types

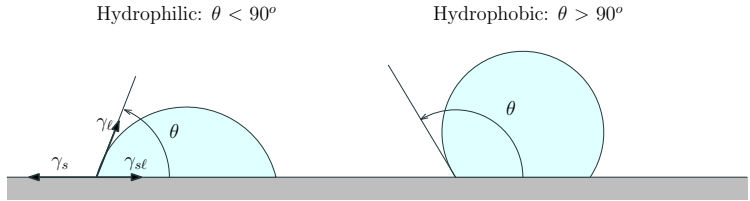

Figure 20: Surfaces classifications

- The angle characterizes the affinity of the solid and liquid;
- Small angle corresponds to a good affinity;
- High surface energy solids (high γ_s) are generally hydrophilic;
- Low surface energy solids (low γ_s) are generally hydrophobic;
- If $\gamma_s > \gamma_{s\ell} + \gamma_\ell$, the fluid totally spreads (no remaining drop).

Surface energy and wetting

- Examples of contact angle on solids of decreasing surface energy.

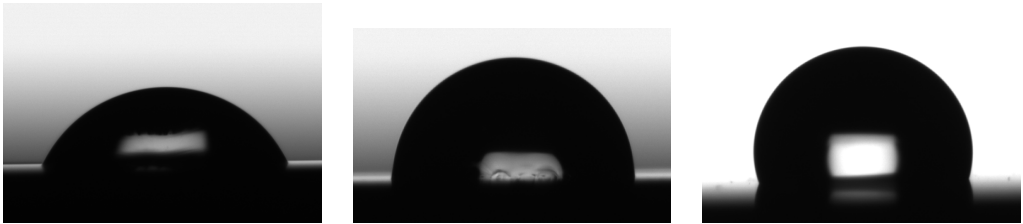

a) b) c)

Figure 21: Sesille water drop on a) Stainless steel b) Silicon carbide c) PTFE

Wetting of a rough/textured surface

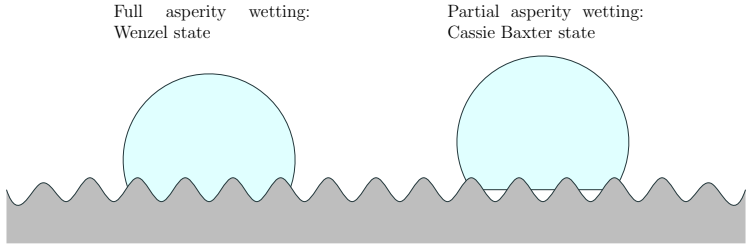

Figure 22: Different wetting regimes of a rough surfaces

- Different wetting regimes of a rough surface
- Wenzel state: the asperities are fully wetted
- Cassie-Baxter state (or fakir state): partial wetting of the asperities
- The most energetically favorable state will be reached

Wenzel regime

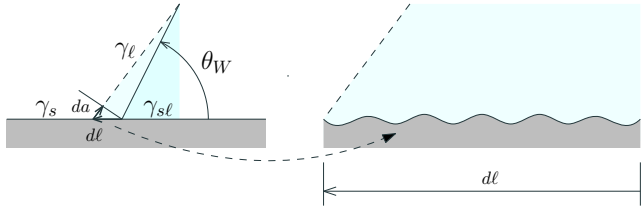

Figure 23: Energy balance at equilibrium

- The real length of the rough surface is linked to the linear length by $d_r\ell = Rd\ell$
- R is a roughness factor ≥ 1.
- Liquid surface energy variation $da\gamma_\ell$
- Solid surface energy variation $-d_r\ell\gamma_s$
- Solid liquid interfacial energy variation $d_r\ell\gamma_{s\ell}$
- Young equation: $\cos\theta_W\gamma_\ell = R\left(\gamma_s - \gamma_{s\ell}\right) = R\gamma_\ell\cos\theta$
- Wenzell relation: $\cos\theta_W = R\cos\theta$

Cassie-Baxter regime

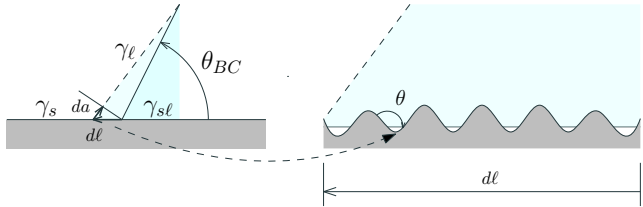

Figure 24: Energy balance at equilibrium

- f is the fraction of solid area wetted by the liquid (horizontally measured).
- Liquid surface energy variation $da\gamma_\ell$
- Solid surface energy variation $-d_r\ell\gamma_s$
- Solid liquid interfacial energy variation: $fd_r\ell\gamma_{s\ell} + (1-f)\,d\ell\gamma_\ell + (1-f)\,d_r\ell\gamma_s$
- Energy balance: $\cos\theta_{CB}\gamma_\ell + fR\,(\gamma_{s\ell} - \gamma_s) + (1-f)\,\gamma_\ell = 0$
- Cassie-Baxter relation: $\cos\theta_{CB} = fR\cos\theta + f - 1$

Example of contact angle on textured surfaces[15]

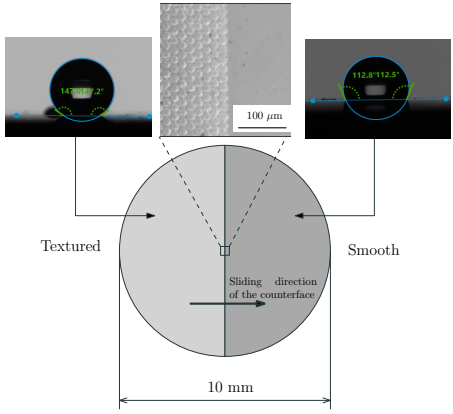

Figure 25: Increase of contact angle by surface texturing

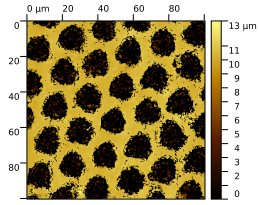

Figure 26: Topography of the rough surface

[15] Hiba Jendoubi, Olga Smerdova, and Noël Brunetière. **"Unexpected Frictional Behavior of Laser-Textured Hydrophobic Surfaces".** In: *Lubricants* 9.3 (2021). ISSN: 2075-4442. DOI: 10.3390/lubricants9030031. URL: https://www.mdpi.com/2075-4442/9/3/31.

Natural superhydrophobic surfaces[16]

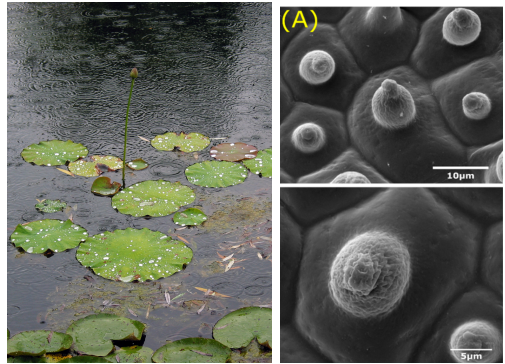

Lotus leaf

Low surface energy material combined with surface roughness leads to superhydrophoic behavior !

[16] Floris Honig et al. **"Natural Architectures for Tissue Engineering and Regenerative Medicine".** en. In: *Journal of Functional Biomaterials* 11.3 (Sept. 2020), p. 47. DOI: 10.3390/jfb11030047. (Visited on 11/23/2020).

Wetting of a rough/textured surface

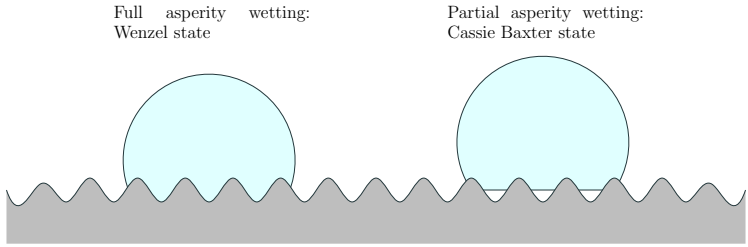

Figure 27: Different wetting regimes of a rough surfaces

- What will be the wetting regime ?
- The most energetically favorable state will be reached.
- It corresponds to the lowest contact angle of the two regimes:
- If $\theta_{CB} < \theta_W$, it will the partial wetting;
- If $\theta_{CB} > \theta_W$, it will the full wetting.

Wetting of a textured suface

- A flat plate with cylindrical cavities of depth h.
- Express the contact angle in the Cassie-Baxter and Wenzel regime
- Application to PTFE and water: $\theta = 110^o$, $r = 4\mu$m, $L = 10\mu$m

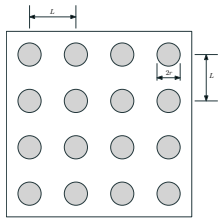

- $\cos\theta_{CB} = \left(1 - \frac{\pi r^2}{L^2}\right)\cos\theta - \frac{\pi r^2}{L^2}$
- $\cos\theta_W = \left(1 - \frac{2\pi r^2}{L^2} \times \frac{h}{r}\right)\cos\theta$

High contact angles require deep texture

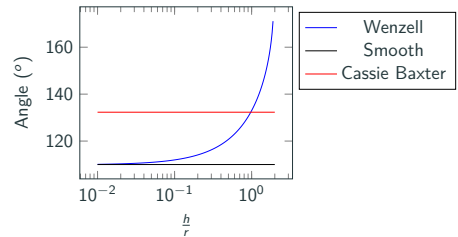

Flow over one cavity[17],[18]

- Navier Stokes solution (CFD - OpenFoam)
- Volume of Fluid + surface tension model
- Calculation of the flow, shear stress, pressure, etc
- Estimation of the apparent slip length
- Effect of the cavity size $\frac{d}{h_f}$ and $\frac{d}{hc}$
- Effect of wetting (one phase flow or two phase flow)

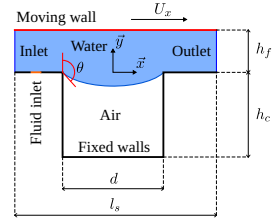

Figure 28: Configuration of the problem

[17] N. Elie. **"Etude théorique et expérimentale des surfaces nano-texturées en régime de frottement lubrifié".** PhD thesis. Université de Poitiers, Dec. 2024.

[18] Nicolas Elie et al. **"Slip Length in Shear Flow Over a Textured Surface".** In: *Tribology Online* 19.4 (2024), pp. 256–265. DOI: 10.2474/trol.19.256. URL: https://hal.science/hal-04664704.

Apparent slip length

- Defined from the averaged speed profile
- Possibility to use the shear stress and the flow rate and compare to smooth channel:
- $Q = \frac{U_x h_f}{2}$ and $\tau = \frac{\mu U_x}{h_f}$
- Thus:
- $\frac{\delta_\tau}{h_f} = \frac{\mu U_x}{\tau_{av} h_f} - 1$
- $\frac{\delta_U}{h_f} = \frac{\frac{U_{av}}{U_x} - \frac{1}{2}}{1 - \frac{U_{av}}{U_x}}$

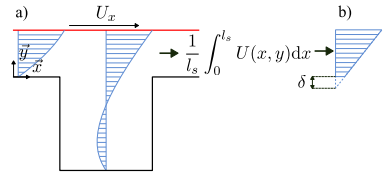

Figure 29: Usual slip length definition from average speed profile

Wenzel wetting regime

- Shear stress decreases when cavity depth increases h_c compared to d and when d increases compared to h_f
- 2 plateaus observed
- First one when $h_c \approx h_f$: formation of a full vortex in the cavity
- Second one when $h_c > d$: the location of the top vortex does not change
- Thus d must be $\leq h_c$ and much higher than film thickness h_f

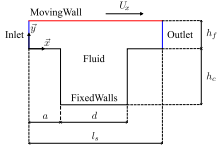

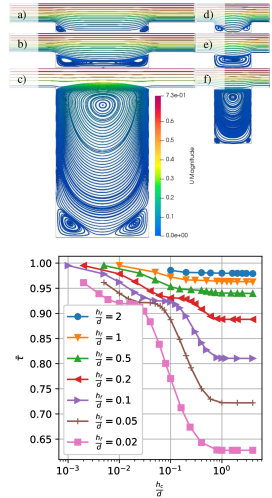

Figure 30: Stream lines for $\frac{hf}{d} = 0.2$ a-c) and $\frac{hf}{d} = 0.2$, Average shear stress

Wenzel wetting regime

- The slip length δ_τ based on the shear stress: monotonous evolution
- Slip length based on the average speed $\delta_U(U_{av})$ has a maximum value.
- Transition occurs when the top of the vortex changes from inside to outside the cavity.
- Thus h_f/d must be maintained in the range 0.2–0.5.

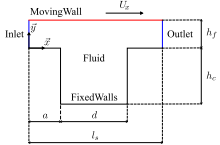

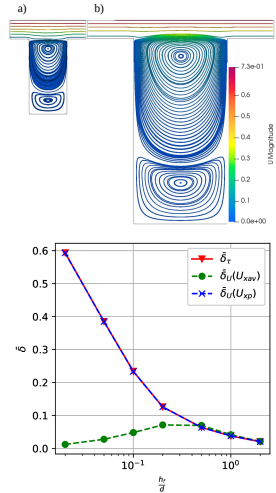

Figure 31: Stream lines for $\frac{hf}{d} = 0.2$ a-c) and $\frac{hf}{d} = 0.2$, slip length for $h_c = 2d$

Cassie Baxter wetting regime

- The viscosity difference leads to a shift of the votex postion / compared to full wetting
- Increasing d/h_f tends to center the votex, as in mono-phase flow.

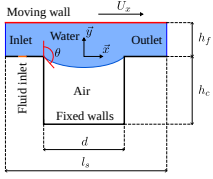

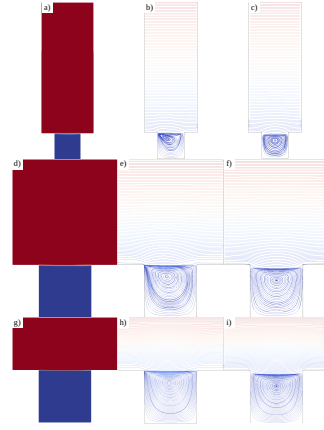

Figure 32: Stream lines in two-phase and mono-phase flow for $\frac{hf}{d} = 5$ a-c) $\frac{hf}{d} = 2$ d-f), $\frac{hf}{d} = 1$ h-j)

Cassie Baxter wetting regime

- $\bar{\delta}_U = \frac{k_1 \frac{d}{h_f}}{k_2^2 + \frac{d}{h_f}^2}$
- $\bar{\delta} \approx \frac{k_1}{k_2^2} \frac{d}{h_f}$, when $\frac{d}{h_f} \ll k_2$ Consistent with literature
- $\bar{\delta} \approx k_1 \left(\frac{d}{h_f} \right)^{-1}$, when $\frac{d}{h_f} \gg k_2$.
- Higher slip with two-phase flow
- Better to have cavities with $\frac{d}{h_f} \approx k_2$

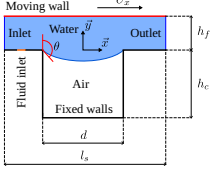

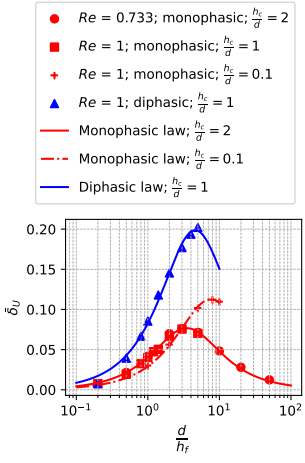

Figure 33: Slip length as a function of d/h_f for Wenzel and Cassie Baxter regimes

Effect of pressure on the liquid - gas interface

- Maximum pressure difference due to Laplace equation
- $p_{lmax} = p_g - \gamma \times \frac{2\cos\theta}{d}$
- if $p_l > p_{lmax}$ the interface will enter the cavity
- Reducing cavity size d is better
- However $\delta \propto d$
- Example with water at 1 MPa in PTFE ($\theta = 110°$), $d = 24$ nm

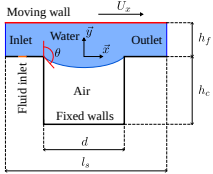

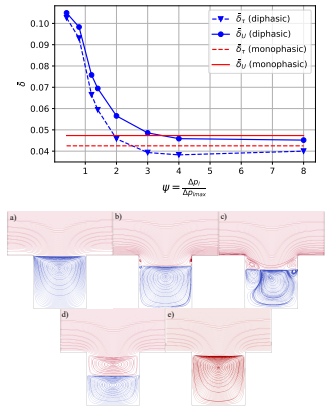

Figure 34: Streamlines for a size ratio $\frac{d}{h_f} = 1, 2$ and for the pressure ratios a) $\psi = 0.4$, b) $\psi = 3$, c) $\psi = 4$, d) $\psi = 8$ and e) monophasic. Evolution of slip length with pressure (top)

Slider bearing

- Slider bearing partially textured at the inlet
- Full texturing = no load

- Pressure generation
- Level of pressure sensitive to the wetting regime and cavity size

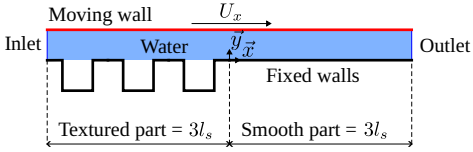

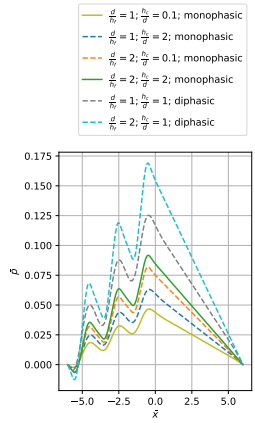

Figure 35: Pressure distribution for different wetting regimes and different cavity sizes

Slider bearing

- The pressure is controlled by the slip length
- Can be incorporated in the Reynolds equation:
- $\bar{p}_{max} = \frac{3\bar{\delta}_U}{2+5\bar{\delta}_U}$
- Allow to model deep cavities

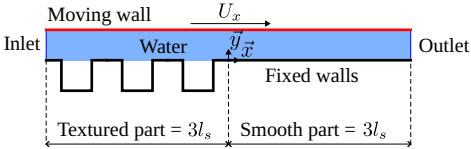

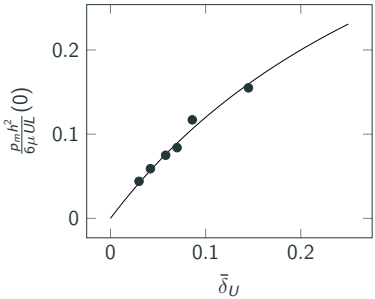

Figure 36: Pressure in the center of the slider as a function of the slip length

Conclusion on deep grooves

- Can surface texturing with deep grooves help in flat on flat lubrication ?
- **Yes** by creating an apparent slip of the liquid **but with conditions**
- Bearing like configurations:
  - Partial texturing located at the inlet only
  - Cavities must have a size with depth $h_c > d$, the width
  - The width d must be as wide as possible with a limit of about 2–4 times the film thickness h_f
  - Cassie Baxter is preferable but the liquid gas interface can enter the cavity at high pressure.

Conclusions

Conclusion on surface texturing in flat on flat lubrication

Shallow grooves $w \gg h$

- Mechanism is hydrodynamic lubrication
- Depth must be similar to the film thickness
- Inlet texturing for bearings
- Un-symmetrical texture for seals

Deep grooves $w < h$

- Mechanism is apparent slip
- Depth must be at least 1 $\times$ width
- Width must be close to 2-4 $\times$ film thickness
- Inlet texturing for bearings

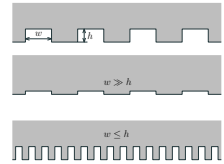

- Both cases can be analyzed with Reynolds equation
- What happens between shallow and deep grooves ?

Thank you for listening

Acknowledgments:

- Colleagues: Dr. J. Bouyer, Dr. P. Jolly, Pr. R. Lucas
- PhD students: Dr. M. Adjemout, Dr. N. Elie
- Companies: Latty, Cetim, IREIS
- Academic partners: Institut Jean Lamour, iRCER
- Projects:
- Microgame ANR-2011-RMNP-00801
- Labex Interatifs ANR-11-LABX-0017-01
- EUR INTREE ANR-18-EURE-0010